

Non-Intrusive Electric Load Monitoring in Commercial Buildings

Leslie K. Norford and Nicholas Mabey
Massachusetts Institute of Technology
Cambridge, MA

ABSTRACT

Increased interest in optimal control, energy scorekeeping and fault detection for HVAC equipment in commercial buildings has focused attention on instrumentation required to obtain the desired data. In this paper we investigate what can be learned from measurements of electrical power at a single point, that of the electrical service for the entire HVAC system. This low-cost measurement has proved in field tests to be capable of detecting the power change when a piece of equipment turns on or off; detecting oscillating equipment power caused by poorly tuned controllers; and detecting suboptimal staging of multiple chillers. Detection of equipment start and stop transitions was strengthened by application of a nonlinear filter that determines the point of median power from a filtering window of user-selected width.

A review of electric motor literature indicated that samples of electrical current taken at slightly faster than twice the 60 Hz fundamental can be used to detect several indicators of incipient motor failure. Tests were initiated to determine whether this technique can be applied to a number of motors on the same circuit.

INTRODUCTION

Non-intrusive electric load monitoring provides information about the operation of HVAC equipment by sampling electric power at a single point rather than by submetering. The technique was developed and applied first to residential buildings by researchers at Massachusetts Institute of Technology, who observed that usage patterns of major residential appliances could be detected by reviewing one-second samples of real and reactive power (2). This paper presents a first look at recent research that focuses on the commercial sector.

While techniques we have developed for commercial buildings have surprisingly little in common with the residential NILM, a brief review of the residential work serves as a useful starting point for our own work. The residential-NILM algorithm defines steady power as three one-second-average data points (each a quartet of real and reactive power on the two branches of residential electrical service) that are constant within an empirically determined tolerance. A start-up transient produces a change that is filtered out until a new, steady power, again defined by three data points, has been established. This efficient, one-pass edge-detection algorithm was designed to ignore power overshoots associated with motor start-ups and to yield a step change in power that was clustered with changes of similar magnitude. Association of step changes with a particular device depended on the tightness of the cluster, with outliers liable to exclusion, and a labeling procedure derived from manufacturer's data or one-time testing of the appliances in a particular building. Field tests of the NILM were generally successful, with the clusters capturing a high percentage of the power changes recorded by submeters (8). Discrepancies could be classified as inclusion within a cluster of step changes that belonged to another

device of similar power, which could be discriminated with such additional information as on-off cycling time; failure to detect devices that exhibited a rate of oscillation between on and off states that was rapid relative to the power-sampling frequency, with thermostated stove burners a prime example; and multistate devices that have been considered by Hart (2) in work subsequent to that embodied in the field-tested load monitors. Hart further noted that devices exhibiting continuously variable powers could not be detected by his algorithms.

The commercial-building application we have investigated posits the presence of an automatic control system responsible for the start-up and shut-down of major HVAC equipment. By limiting, at this stage of our research, the role of the NILM to that of support for an automation system, we have access to important information, namely the identity of a device and the precise time at which the control system initiates a start-up or shut-down signal. Therefore, changes in power can be assigned to the device receiving the control signals, and the strength of the association can be tested statistically. There is no longer a need to make an association on the basis of clustering procedures that must be at once sufficiently inclusive to lower the risk of ignoring step changes caused by the appliance in question, and sufficiently exclusive to discriminate appliances that have comparable values for clustering parameters. The primary advantage of relying on start-stop signals rather than clusters for device identification is enhanced fault detection: a change in power indicative of a fault might fall outside a cluster, but, with little or no ambiguity, can be related temporally to a control signal.

DESCRIPTION OF EXPERIMENT

To provide initial experience in monitoring HVAC devices at a central location, we installed a Watt transducer on the 480V 3 phase electrical service that provides power for HVAC equipment in two campus buildings. The equipment includes two identical 500-ton centrifugal chillers and associated chilled water (50 hp) and condenser water (40 hp) pumps; two large supply fans with adjustable-speed drives (125 and 100 hp); and a number of smaller pumps and fans; maximum total power for the system was about 1000 kilowatts. One-second average samples of the Watt transducer's output were stored on a portable computer.

DETECTION OF ON-OFF TRANSITIONS AND DETERMINATION OF POWER LEVELS

It is important for a control system to receive confirmation that HVAC components have indeed responded to on-off control signals. Such would not be the case if the device were inadvertently placed under manual control or if there were an electrical fault. Traditionally, a control system relying on electrical confirmation of response to on or off signals has made use of a single current transducer per device. We have assessed whether a NILM could perform the same task, without need for individual current transducers.

The ability of a NILM to detect device transitions is limited by the magnitude of the unexplained electrical power variations measured at the HVAC electrical service distribution panel or other central location. If the "noise" is large, then only larger devices can be observed. If the signal can be completely explained, or nearly so, then very small devices can be detected. Figures 1 and 2 show data that include large-amplitude oscillations that will be discussed later and on-off transitions of HVAC equipment. Standard deviations during periods of nearly steady power were about 5 kW. This remarkably small number, less than 1 percent of the total, indicates that pumps and fans of moderate or large size should be detected readily, while small return and exhaust fans would not be found easily.

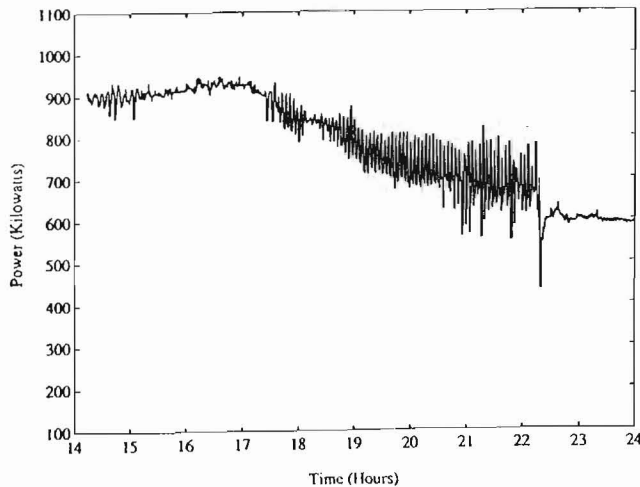


Figure 1. Electric power at the building HVAC service entrance, July 22, 1991. A poorly tuned chiller controller operating under low-load conditions caused the large power oscillations.

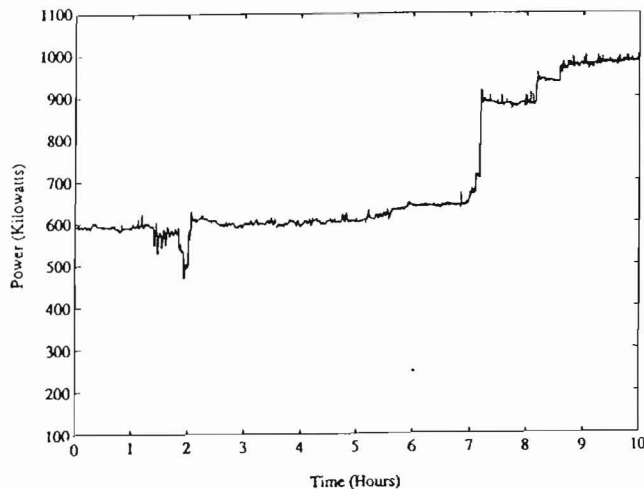


Figure 2. Electric power at the building HVAC service entrance, July 23, 1991. A chiller and associated pumps were turned on at 7 am.

To quantify the resolution that can be obtained with a 5 kW standard deviation, we apply statistics appropriate for testing hypotheses of differences between two means. We show in Table 1 the minimum difference in means that will reject the hypothesis that there is no change, at the 5% level of significance. There is large benefit in increasing the sample size

from 5 to 10, at which point an HVAC device drawing more than 5 kW can be detected at the 5% level of significance.

Table 1 Confidence intervals for testing differences in means, based on 5 kW standard deviation.

Sample size	Minimum difference in means (kW)
5	9.8
10	5.3
15	4.1
20	3.4
25	3.0
30	2.7

Pumps

Figure 3 illustrates four on and off transitions for a 50 hp condenser-water pump, which was tested at a time when the other condenser pump was in constant operation. The increase in system power when the pump is running is large relative to the 5 kW standard deviation and periods of pump operation can be visually discerned. However, the figure shows that the pump motor is more complicated than a simple two-state device with a motor start-up power surge, for several reasons:

1. After start-up, there is a long period of slowly decreasing power, during which fluid pressures in the water loop are approaching equilibrium. The pump just started must reach a balance with the pump already running, at which time each pump is drawing less power than either would if running alone.
2. After the test pump is turned off, the remaining pump, still in operation, is subjected to a larger load and its power increases. There is only a narrow window in time--about 5 seconds--during which to establish the power change of the test pump at shutdown; a larger averaging period will be affected by the increased power of the second pump. We have observed similar behavior with the two chillers.
3. There are periodic spikes as large as 20 kW magnitude, which may be due to variable-speed-drive fan controllers responding to set-point changes.

To detect on-off transitions and compute the difference in mean powers before and after the transition, we require a filter that removes impulses but preserves edges. This filter should remove both the periodic spikes and the spikes associated with motor dynamics. While a large sample size, or window, produces smoother power readings, the window must be narrow enough to detect the trough in power at shutdown that can disappear when a second, similar device is running. We have evaluated three types of filters: the three-point sliding window, with user-assigned tolerance defining steady power, as developed by Hart (2); a filter that integrates data after a change exceeding a user-defined tolerance, to determine whether the triggering data were due to an impulse (no change in before and after integrations) or a step; and a median filter with user-defined window. It is important to note that all of these filters differ from linear filters that respond to frequency and therefore are poorly suited to distinguish impulses and edges, both of which have similar frequency content.

For our application, it was difficult to set the filter tolerance for the residential-NILM filter. A tight tolerance, 5 kW or less, caused the average to be reset at most spikes, which were therefore treated as significant events, albeit with little or no change in power. A loose 15 kW tolerance, on the other hand, not only averaged the spikes but ignored devices of magnitude less than 15 kW. The larger tolerance also smoothed the dip and subsequent rise in power at shutdown that must be preserved as

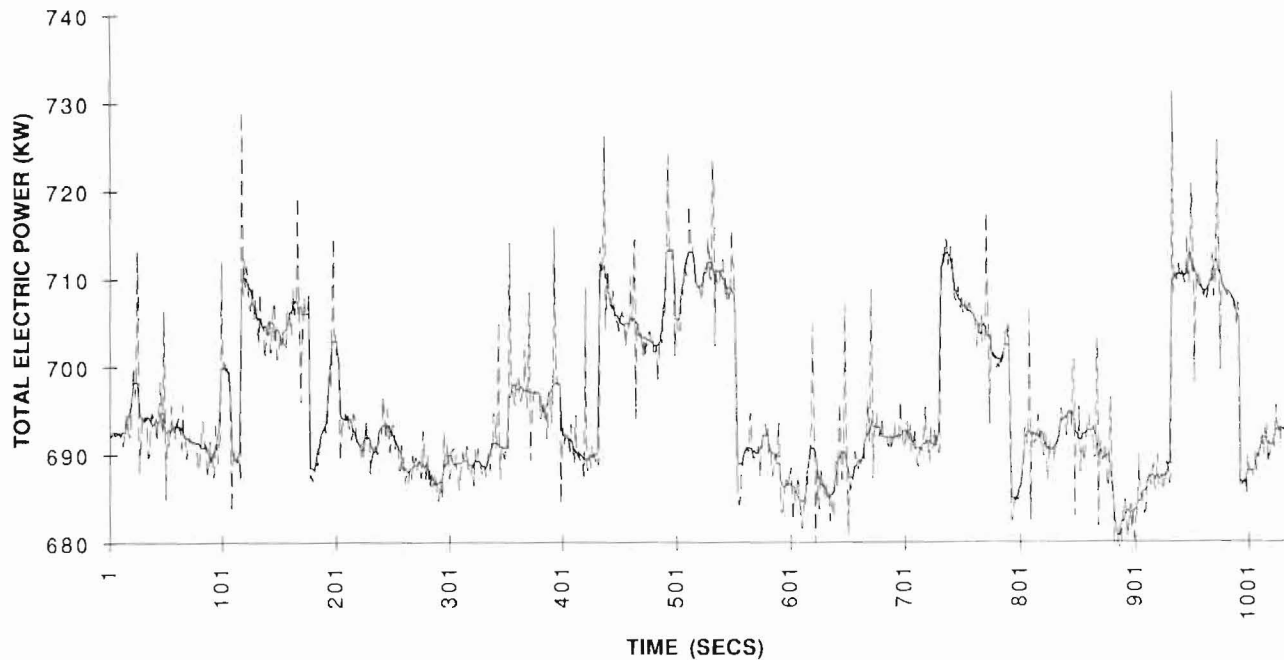


Figure 3. Changes in electric power at the HVAC service entrance due to switching a condenser-water pump on and off. Noise in the raw data, shown as a dashed line, is removed by the median filter.

the true indication of the power change associated with the pump, and flattened the gradual decrease in power after start-up. We did not adjust the width of the window, which determines the minimum event duration that can be detected. A narrow window can pick up very short events and separate events that are nearly simultaneous in time, but the small sample size produces larger uncertainty in the difference in means. The maximum window width permitted by the data, as noted above, appears to be about 5 seconds.

The integral filter that we developed was better able to discriminate against the impulses. The integration function and comparison of results before and after an impulse amount to the type of automated post-processing that Hart's method requires. The comparison function demands a value for acceptable agreement, another parameter that is use-specific.

The median filter is one of a class of nonlinear filters that incorporate a sorting function (5). It sorts the data points in its window and preserves the median before sliding over one point and repeating the process. This filter removes impulses, which appear in the window as one or two points of very large or small power that have little or no effect on the median. The sort can be time-consuming but as compensation offers the significant benefit of requiring only a single parameter, the width of the window, which can be determined readily by the minimum temporal feature of interest. We used a window of 11 points. Figure 3 shows the remarkable results of the median filter as well as the raw data.

The median filter and our integral filter gave comparable standard deviations, as indicated in Table 2, and the two sets of filtered data (not shown in Figure 3 for the integral filter) appeared nearly identical. With an 11 point window, the median filter tended to slightly underestimate the change in power associated with the on transitions, a systematic effect that had minimal impact on the standard deviation. The Res-NILM filter, applied to raw data, gave erratic results manifested in large standard deviations, because a tolerance large enough to smooth noise (5 kW) also

smoothed the dynamics, described above, that were present after start-up and shut-down.

We applied the Res-NILM filter to data that were passed through the median filter and have therefore been stripped of impulses. Figure 4 shows the results, which are quantified in Table 2. With the tolerance as set, Hart's filter waited until the start-up fluid dynamics had settled before establishing a new level. Similarly, at shutdown, it clipped the narrow drop in power that occurs before the remaining pump picked up the load. The start-up power, therefore, represented more of an equilibrium value than that determined by the median filter alone and was consistently lower. Also, the standard deviation for the combination of the two filters exceeded that of the median filter alone, perhaps because the total power signal may have changed for other reasons during the time required for the pump to reach equilibrium. The growth in the standard deviation argues against the combination of filters, because it reduces the likelihood of detecting equipment faults. Note from Table 2 that the standard deviation for shutdowns was also larger for the two-filter case.

Fans

We recorded total HVAC electrical power at times when a 125 hp supply fan was turned off and on twice, followed by one off-on cycle for a 100 hp fan. Both fan motors are controlled by adjustable speed drives (ASDs). The raw data are shown in Figure 5, while Figure 6 shows filtered electrical power. There were no power spikes at start-up, because the ASD electronics include a soft-start feature. The fans did not interact with other fans and, unlike the pump data, there was no evidence of increase in power shortly after shutdown. Power levels dropped after start-up, when the frequency established by the ASD was reduced from its initial value of 60 Hz to that required by the fan to maintain supply duct static pressure at set point. For these data the median filter preserved the ramping of power characteristic of a soft start and our procedure for extracting a change in power level slightly underestimated the start-up power. As indicated in Table 3, there was no clear-cut winner among the filters. The median filter produced standard deviations comparable to the

Table 2 Changes in electrical power due to turning a pump on and off, as determined by application of three different filters.

Trial	Median (11 point)		Integral (10 kW)		Hart (5 kW)		Median + Hart	
	On	Off	On	Off	On	Off	On	Off
1	18.2	-17.6	24.2	-19.8	18.4	-16.5	15.6	-14.5
2	20.9	-18.2	23.5	-16.7	25.1	-25.9	20.6	-20.5
3	18.8	-17.3	22.4	-19.6	15.2	-18.1	16.0	-18.8
4	21.7	-20.3	25.0	-18.7	29.6	-24.7	24.3	-19.0
Average	19.9	-18.3	23.8	-18.7	22.1	-21.3	19.1	-18.2
Std Dev	1.7	1.4	1.1	1.4	6.5	4.7	4.1	2.6

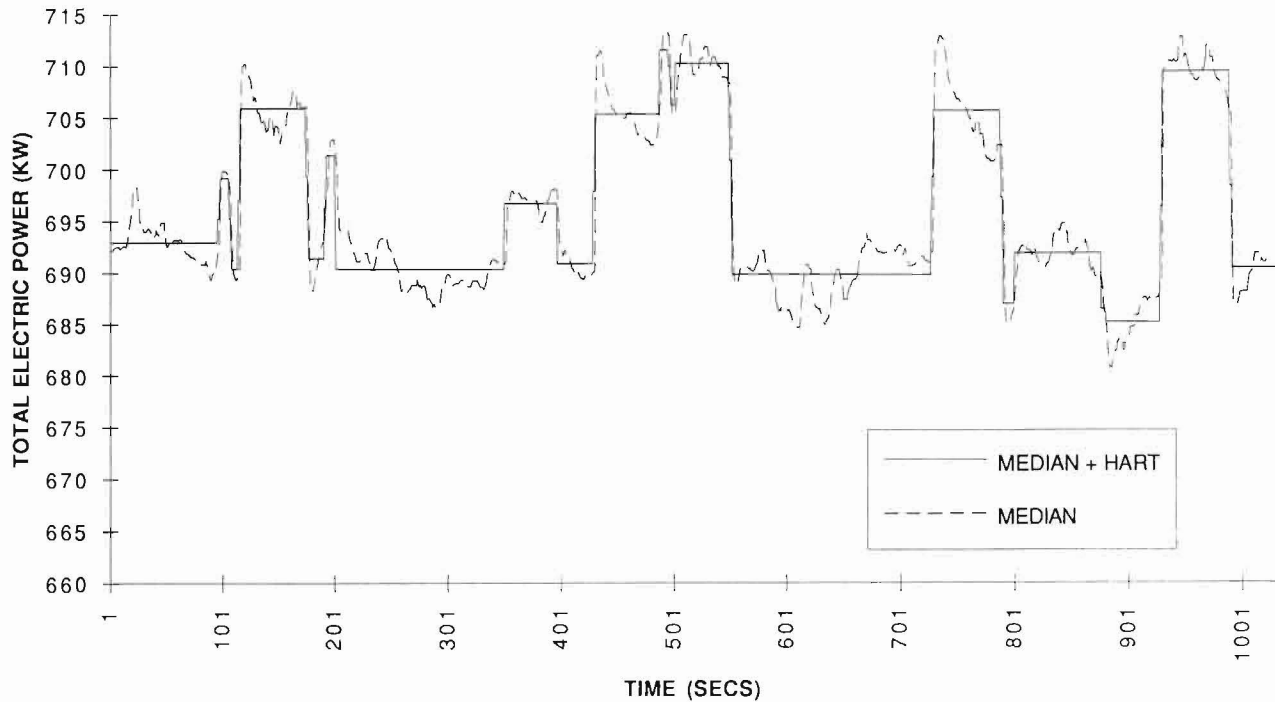


Figure 4. Condenser pump operation, as shown by the median filter alone and by successive application of the median filter and an averaging filter, developed by Hart (2) that accentuates changes in power level. A 3 kW trigger was used with Hart's filter.

integral filter and Hart's filter, both of which required more tuning and therefore are not as robust.

FAULT DETECTION

This paper does not attempt to catalogue faults by HVAC component or system. Recent papers (4, 6) describe faults in

ventilation systems. Rather, we describe particular types of faults that our non-intrusive metering found and assess additional applications that rely on more rapid sampling.

High Controller Gains

Figure 1 shows large power oscillations with a peak-to-peak amplitude, about 150 kW, that exceeds the rated power of any device except the chillers. This simple, heuristic identification

Table 3 Changes in electrical power due to turning fans on and off, as determined by application of three different filters. Summary statistics are for the first two trials, which involved the same fan.

Trial	Median (11 point)		Integral (10 kW)		Hart (5 kW)		Median + Hart	
	On	Off	On	Off	On	Off	On	Off
1	48.2	-27.1	57.4	-28.2	52.8	-30.7	51.1	-30.2
2	45.5	-35.8	53.1	-32.8	49.0	-39.1	52.2	-42.0
3	50.1	-34.0	60.6	-38.2	60.7	-43.8	57.4	-37.0
Average	46.9	-31.5	55.3	-30.5	50.9	-34.9	51.7	-36.1
Std Dev	1.9	6.2	3.0	3.3	2.7	5.9	0.8	8.3

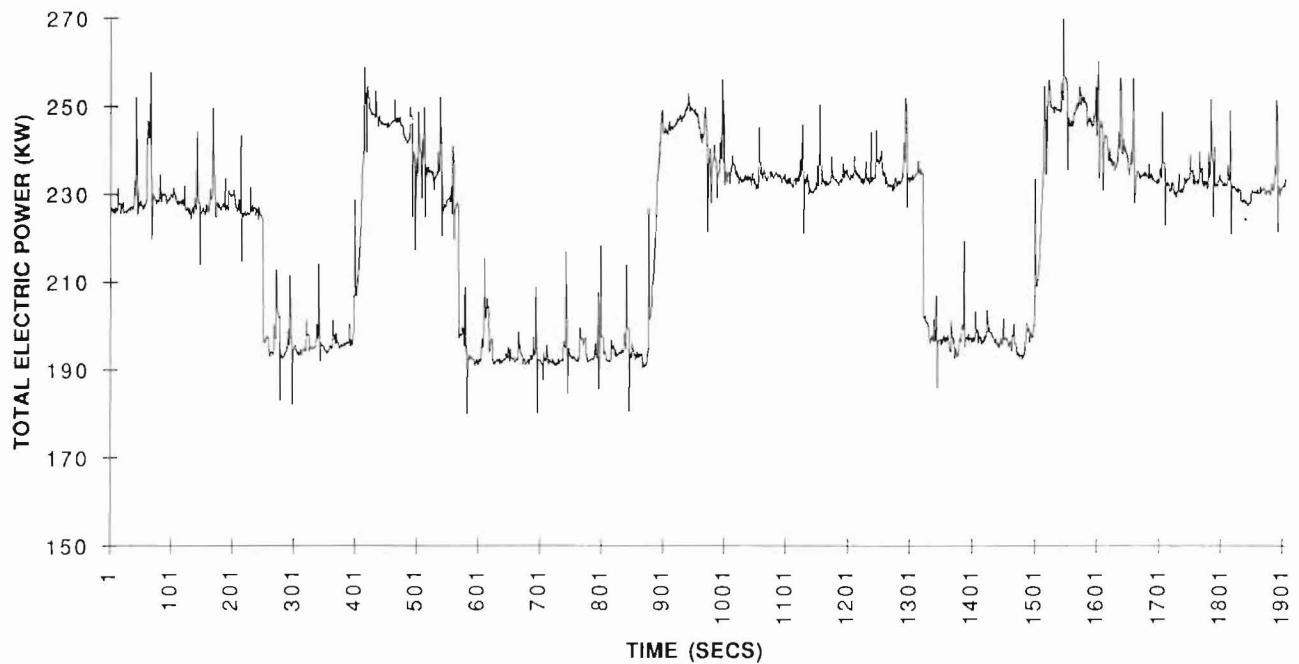


Figure 5. Start and stop transitions for two large supply fans.

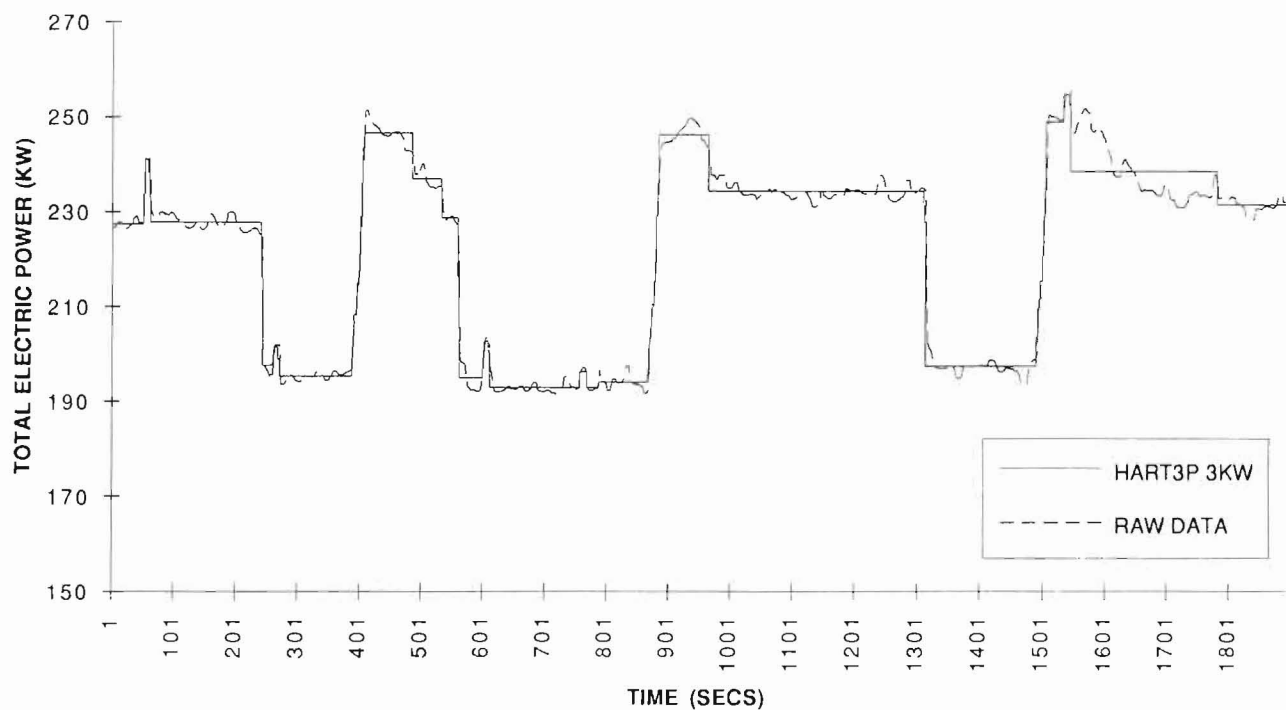


Figure 6. Start and stop transitions as clarified by the median filter alone and by successive application of the median filter and Hart's filter.

relies on a list of equipment and rated powers as information to supplement power measurements.

Oscillations started when the total power dropped and stopped when the power rose or, as shown in Figure 1, when a piece of equipment identified from the control signals as one of the two chillers was turned off. The data led us to conclude that

oscillations occurred at times when the chillers were lightly loaded and were due to poorly tuned controller gains. The chillers are operated to maintain chilled water temperature, with inlet vanes controlling the flow of refrigerant. With control gain too large, the vane position is varied too much, causing unnecessary equipment wear, and the chilled-water temperature error oscillates from positive to negative values. A Fast-Fourier-

Transform of the data showed a strong spike at the frequency associated with the four-minute sample time used by the chilled-water temperature controller.

Switching Multiple Chillers

Optimal control strategies have been developed by Braun et al (1) and detection of power deviations from optimal conditions has been explored by Pape et al (7). The amount of information required for optimization has deterred its acceptance by industry and building owners. A NILM offers a lower cost, somewhat less informative, but still powerful approach by providing a basis for identifying what is clearly not correct, even if it is not possible to establish how to achieve what is optimal. The earlier discussion of chiller oscillations is one example of this approach.

A second example concerns switching among multiple chillers and chilled water pumps. Braun et al (1) showed that optimal switch points can be defined as producing no discontinuity in system coefficient of performance (COP), as shown in Figure 7. That is, if a second chiller is turned on at too low a cooling load, COP will drop and power will rise. Power will drop if it is turned on at too high a cooling load. Similarly, power will fall if the second chiller is turned off too late, that is, when the cooling load has dropped below the optimal switch point. The same argument can be made for pump switching.

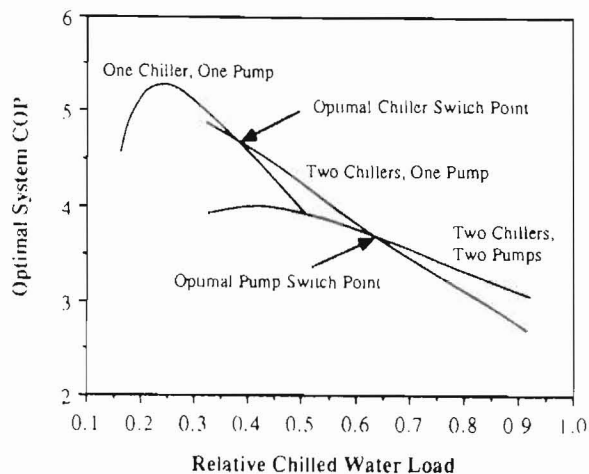


Figure 7. Optimal switch points for a two-chiller, two-pump system, taken from Braun et al (1). Optimal switch points result in no change in power, while suboptimal switching shows power changes. A non-intrusive load monitor can reveal such changes.

Our data in Figure 1 show that the second chiller was turned off after the optimal cooling load switch point had been passed. Mean power dropped by about 100 kW, indicating that the combined power for both chillers exceeded the optimum by that amount for some period of time leading up to shutting down the second chiller. This information, if detected by a NILM, can guide plant operators toward more efficient plant operation.

A type of chiller staging not observed experimentally in this study concerns when to turn on the first chiller. At issue is how large a cooling load can be met by the ventilation system bringing in 100% outdoor air, and how much fan power is required. Traditional practice has maintained the supply air temperature at a fixed value, forcing the chiller on when the outside temperature approaches this set point (with a small decrement due to temperature rise across the fan). Fan power will therefore stay the same immediately after the chiller is turned on and the chiller will be running at relatively low load. Alternatively, the supply

air temperature could be allowed to float upward, with the chiller turned on when the fan is running at maximum load or (less likely) the increase in fan power exceeds the power drawn by the chiller. The latter case is exactly the same as the problem of staging the second chiller and the NILM will tell whether there has been a telltale net increase in power. In the former case, the fan alone can be used until its speed control signal reaches a maximum. The availability of this control signal provides a low-cost method of optimizing the start-up of the lead chiller.

Electric Power for Equipment Subject to Variable Loads

Non-intrusive measurement of electrical power at times between start up and shut down is difficult for equipment that draws a varying amount of power. A list of such equipment includes variable-speed devices and fixed speed equipment subject to variable loads. In these cases, it may be necessary to correlate power with another variable that can be measured for each piece of equipment. Norford and Little (6) presented data for an ASD centrifugal fan that showed power, when correlated with the ASD control signal (which, as a control signal, is available to a non-intrusive meter at essentially no cost), was less sensitive to duct pressure variations than when power was correlated with airflow. They supported this observation by noting that a typical fan curve displays lines of constant mechanical power that, for moderate to large flows, nearly parallel lines of constant fan speed.

A centrifugal pump powered by an induction motor operating at fixed electrical frequency shows the same insensitivity of power to changes in pressure, at least in the vicinity of the design point, as does an ASD fan when power is correlated with speed control signal. Therefore, power is not a useful diagnostic of small pressure changes.

Motor Faults

Almost all of the HVAC facility managers interviewed as part of this project indicated that the failure of motors used to drive pumps, fans, or compressors was a significant problem. Motor failure was described as unanticipated and disruptive. Our review of the literature of electrical machinery has shown that electrical monitoring is one method of assessing the condition of motors to prevent unanticipated failures.

Tavner and Penman (9) catalogued failure mechanisms in electrical machines: machine enclosure (cooling system, bushings and electrical connections); stator core (laminations and frame); stator windings; rotor body; rotor windings; bearings and seals; commutators, slip rings and brush gear; and auxiliary equipment. No probabilities of failure were assigned to the categories. They then described monitoring techniques based on electrical measurements, chemical measurements, vibration, and temperature. They noted that machines rated at less than 20 kW usually do not warrant the cost of dedicated monitoring.

Monitoring the electrical current drawn by the stator of an induction motor is one technique described by Tavner and Penman for detecting rotor faults. Rotor defects are of particular interest because rotor imperfections can deteriorate under the large electrical, mechanical and thermal stresses present in the rotor. Rotor faults cause electromagnetic fields that modify the current drawn by the stator and produce torques that cause vibrations. In frequency space, rotor-bar defects yield stator-current harmonics displaced by twice the slip frequency from the fundamental.

The technique has also been used to detect damaged gear boxes and rotor eccentricity due to bearing wear. Liu (3) examined, via theory and experiment, stator current indications of eccentricity in

the airgap separating stator and rotor. She distinguished two types of eccentricities: fixed deviations from perfect concentricity, due to mounting the rotor shaft slightly off center; and dynamic deviations, due to either an out-of-round rotor or bearing damage, that yield an airgap which, at any point, will vary as the rotor turns. Liu found:

1. Static eccentricity drops the current at the fundamental frequency, by an amount difficult to discern experimentally due to unmodeled and confounding fluctuations in the 60-Hz current.
2. Dynamic eccentricity yields a single frequency sideband, lower than the fundamental by twice the slip frequency.
3. Static and dynamic eccentricities in combination produce a series of harmonics. Liu found in practice that the frequencies of the harmonics were accurately predicted by her motor model while amplitudes were less accurately characterized. Experimentally observed harmonics in the absence of deliberately introduced eccentricities were ascribed to voids in the rotor or rotor-bar fractures, an observation consistent with Tavner and Penman's application of current monitoring. Because the harmonic amplitudes were difficult to predict, Liu concluded that detection of motor faults requires analysis of how harmonics change over time.

Thomson et al (10), in a similar project, reported on current and vibration monitoring to detect airgap eccentricity. Frequencies of interest were higher than those of concern to Liu. Thomson looked at harmonics caused by the rotor slots and present even in a healthy motor, and how these harmonics are modified due to eccentricities. He found:

1. An increase in static eccentricity from 0 to 60% had little effect on the magnitude of the principal slot harmonic. A further increase to 80% produced a much greater enhancement of stator current. Liu, by contrast, predicted a decrease in the stator fundamental current due to static eccentricity. Thomson noted that static eccentricity induced increases in harmonics on either side of the principal slot harmonic.
2. Deliberately introduced dynamic eccentricity had little effect on the principal slot harmonic but substantially increased the sidebands. These sidebands, along with the principal slot harmonic, were in practice shifted by changes in the frequency of the incoming current, making on-line detection more difficult. Thomson noted that work was underway to relate the magnitude of the frequency components to the severity of the eccentricity.

Stator current analysis requires that data be taken at a frequency slightly greater than twice the largest harmonic of interest, to satisfy the Nyquist criterion. Liu took 200 Hz as an upper limit, sampled at 666 Hz, and low-pass filtered the data with a sixth-order Butterworth filter to prevent aliasing. For a NILM, the issue is one of performing the frequency analysis at a point remote from any particular device. Motor fault detection by current analysis is not comprehensive--that is, not all types of faults can be detected. But successful current analysis by the NILM is a very low cost feature when considered as a supplement to such functions as the previously described load detection.

We have analyzed electrical current harmonic spectra in a laboratory setting, for combinations of three motors. Two were fractional-horsepower single phase motors and the third a larger three-phase motor. The shaft of one of the single-phase motors was connected via a belt under tension to another pulley, subjecting the rotor to a torque that would tend to create eccentricity. As shown in Figures 8 and 9, the presence of the belt resulted in pronounced changes in the spectra, with

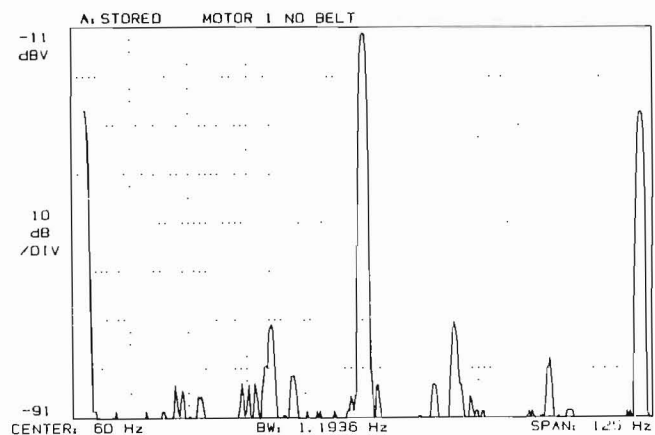


Figure 8. Motor harmonic spectrum.

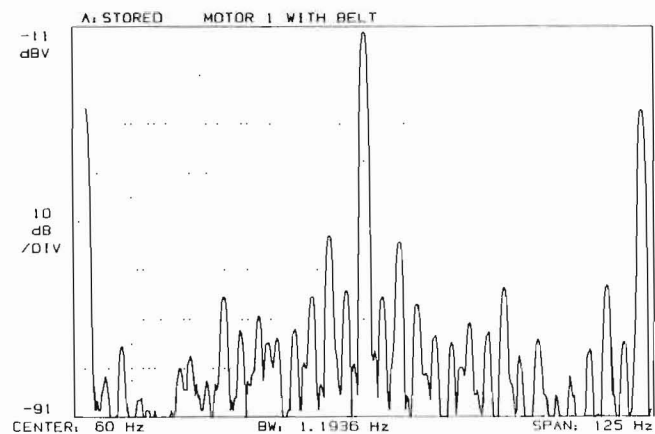


Figure 9. Motor harmonic spectrum, with belt attached to the shaft of a second motor. The belt, under tension, creates a torque on the shaft that causes rotor eccentricity, as revealed in the sidebands to the fundamental signal.

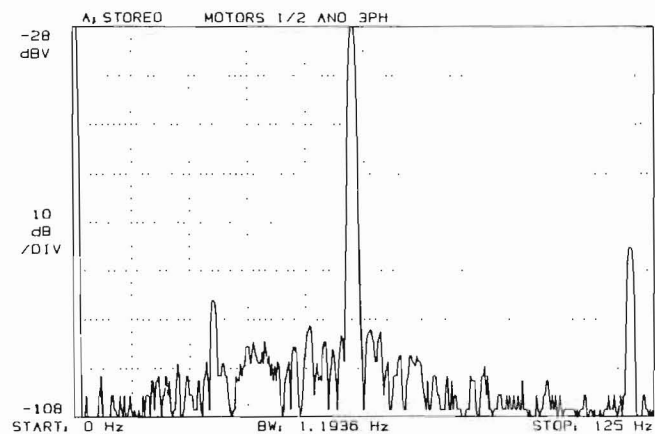


Figure 10. Harmonic spectra for three motors. The larger third motor obscures the sidebands associated with the smaller motor.

prominent sidebands located at about 7.5 Hz above and below the fundamental. These sidebands were also visible when both of the single-phase motors were operating concurrently. However, when the third, larger motor was then turned on, its harmonic spectrum obscured the sidebands associated with the smaller motor, as indicated in Figure 10. As a next step, we will take current spectra in our test building and determine whether sidebands can be observed when motors are run individually (as in many cases they could be, during periods of time when the remaining HVAC equipment was shut down) or simultaneously.

CONCLUSION

Non-intrusive electric load monitoring has been shown, in a test building, to be capable of detecting from a single location the on and off electrical transients associated with fans, pumps and chillers. Centralized monitoring also revealed a poorly tuned chiller controller and suboptimal switching among two chillers. Laboratory tests indicate that the monitor may be able to identify motor faults via analysis of electrical current spectra. While further work is needed, particularly with motor fault detection, the encouraging results point to an era of less expensive, more capable load monitoring and fault detection equipment.

ACKNOWLEDGMENT

The authors gratefully acknowledge financial support and technical advice provided by the Electric Power Research Institute and Johnson Controls. Ruel Little installed the data logger used in the field studies. Andrea Kendrick and Alice Yates assisted in the collection of data. Jim Kirtley, Steve Leeb, Richard Tabors and George Verghese provided guidance during the course of the research.

REFERENCES

1. Braun, J. E.; Klein, S. A.; Mitchell, J. W.; and Beckman, W. A. 1989. "Applications of optimal control to chilled water systems without storage." ASHRAE Transactions Vol. 95, Pt.1.
2. Hart, G.W. 1991. "Nonintrusive appliance load monitoring." Department of Electrical Engineering, Columbia University. Draft manuscript.
3. Liu, S. 1990. "Detection of airgap eccentricities in squirrel cage induction motors using stator current measurements." M.S. Thesis, Department of Electrical Engineering and Computer Science, Massachusetts Institute of Technology, Cambridge, MA.
4. Liu, S. T. and Kelly, G. E. 1989. "Rule-based diagnostic method for HVAC fault detection." Proceedings of Building Simulation '89, The International Building Performance Simulation Association. Vancouver, B.C., Canada
5. Karl, W. C.; Leeb, S. B.; Jones, L. A.; Kirtley, J. L.; and Verghese, G.C. 1990. "Applications of a class of nonlinear filters to problems in power electronics." Record of the IEEE Power Electronics Specialists Conference.
6. Norford, L. K. and Little, R. D. 1992. "Fault detection and load monitoring in ventilation systems." Draft to be submitted for publication in ASHRAE Transactions.
7. Pape, F. L. F.; Mitchell, J.W.; and Beckman, W. A. 1991. "Optimal control and fault detection in heating, ventilating, and air-conditioning systems." ASHRAE Transactions, Vol. 97, Pt.1.
8. Tabors Caramanis and Associates. 1992. "Nonintrusive load monitoring: draft final report." Electric Power Research Institute, Palo Alto, CA.
9. Tavner, P. J. and Penman, J. 1987. Condition Monitoring of Electrical Machines. Research Studies Press, Exeter, England.
10. Thomson, W.T.; Cameron, J.R. and Dow, A.B. 1988. "On-line diagnostics of large induction motors." Vibrations and Audible Noise in Alternating Current Machines, Belmans, R.; Binns, K.; Geysen, W.; and Vandenput, A., eds. Kluwer Academic Publishers.